Enhancing Smartphone Indoor Localization via Opportunistic Sensing

Kaikai Liu
Computer Engineering Department
San Jose State University (SJSU)
San Jose, CA, USA Email: kaikai.liu@sjsu.edu

Di Wu
Hunan University
Changsha, China
Email: dwu@hnu.edu.cn

Xiaolin Li
Electrical and Computer Engineering
University of Florida
Gainesville, FL, USA Email: andyli@ece.ufl.edu

***Abstract*—Using a mobile phone for fine-grained indoor localization remains an open problem. Low-complexity approaches without infrastructure could not achieve accurate and reliable results due to various restrictions. Accurate solutions relying on dense anchor nodes are inconvenient and cumbersome in deployment. The anchor blockage problem would further reduce the effective coverages. In this paper, we investigate the problems associated with improving indoor localization of a mobile phone via opportunistic anchor sensing, a new sensing paradigm leveraging multiple anchors without minimum number or constellation requirement. One key motivation is that the location results could be improved by exploring more data types rather than deploying more anchor nodes. To enable this high scalability and accuracy design, we leverage low-coupling hybrid ranging by our low cost anchor nodes with centimeter-level relative distance estimation. Activity pattern extracted in local smartphone is utilized for accurate displacement and direction estimation. Finer localization resolution could be achieved with sufficient anchor access. We introduce the delay-constraint robust semidefinite programming in trilateration calculation with the potential of centimeter-level location resolution. We conduct extensive experiments in various scenarios. Compared with other approaches, opportunistic sensing could improve the location accuracy, scalability as well as robustness under various anchor accessibilities.**

***Index Terms*—Localization, Smartphone, BLE, Acoustic.**

I. Introduction

Ubiquitous smartphone and location information are enabling new features of location-based services (LBS) around local navigation, retail recommendation, proximity social networking, and location-aware advertising. Recently, the focus is also shifting geographically from outdoor to indoor, where we spend most money, meet friends, work and do business.

The indoor location market will be more enormous than outdoor, since we spend more than 80% of time indoor in our daily activities, e.g., working, shopping, eating, at the office, at home. Technologically, outdoor localization techniques cannot be directly moved to indoor. Satellite based localization, e.g., GPS, has been one of the most important technological advances of the last half century. No matter how good the systems get in outdoor, its accuracy, coverage and quality deteriorate significantly in small-scale indoor places. Emerging techniques using existing infrastructure, e.g., WiFi access point, Cellular tower, could only achieve limited accuracy, or need extensive war-driving and calibration [1], [2]. Other accurate approaches rely on the deployment of additional infrastructure [3], [4], [5], [6], e.g., dense anchor nodes. These approaches have a high requirement on the minimum anchor number, e.g., at least three anchors for 2-D trilateration. The highly dynamic and mobile setting, where humans are essentially moving, presents further challenges for existing solutions either using existing infrastructure or self-deployed anchor network. There exist inherent tradeoffs between the localization accuracy and the deployment complexity. Existing low-accurate or high-complex indoor localization solutions in a mobile phone call for significant innovations in balancing the accuracy and complexity.

In this paper, we propose a highly accurate and scalable mobile phone localization system via opportunistic anchor access. The key motivation of our design is originated from the problem associated with acoustic anchor-based solution [4] with centimeter-level accuracy, i.e., the acoustic anchor can be easily blocked, and it is hard to access minimum *three* anchors for trilateration in real environments. Deploying more anchor nodes in not economically practical and hard to manage, especially maintaining the high timing accuracy of the complex network. Leveraging multi-modal types instead of deploying more nodes are a good direction in improving the efficiency and utilization. However, existing hybrid solutions mainly focused on meter-level coarse-grained applications, and these approaches do not match well with fine-grained approaches. For example, combining meter-level results with centimeter-level results would downgrade the overall performance instead of improving. Transforming the high level system design goal into a practical working system poses significant challenges: (1) How can we improve the location accuracy even with limited anchor nodes? (2) Will our system adapt to higher accuracy with more data types or better anchor accessibility? This paper addresses these challenges, and prototypes the system via *opportunistic anchor sensing*. Testbed results confirm our design goals that could adapt to different anchor coverage and service quality requirement with high scalability, e.g., from only one node to multiple nodes with multi-modal data. We believe this could be a practical approach to achieve fine-grained localization results with very low hardware requirement and deployment cost, also scalable for applications with fine-grained resolution demand, e.g., indoor accessibility assistance for the visually impaired, and robotic navigation.

II. System Overview

A. Motivation

Unlike [4] that requires minimum *three* anchors, the approach proposed in this paper works under different "anchor" coverage environments, i.e., scales from only one "anchor" rather than the minimum *three* anchors. **Lowering the minimum anchor number requirement** is essential for the system scalability and low-complexity. For applications with limited budget of anchor deployment, deploying several anchor nodes (less than three) could still achieve significantly better accuracy than anchor-free solutions. When the number of deployed anchors increases (large than three), our proposed algorithms can adapt to high accuracy results contributed by the additional anchors. With this flexibility, location service operators could select configurations that suit various service quality requirements.

When only one anchor node is accessed, traditional approaches cannot perform trilateration. The only obtainable error surface is like a ring shape, with the distance as the radius and the RSS ranging accuracy (meter-level) as the width. To improve the location accuracy in this case, we need to leverage additional sensing data without adding additional nodes. Three possible sensing sources include: 1) the ranging information for the anchor node and smartphone pair; 2) relative angle information; 3) displacement and moving direction of the target. If multiple anchor nodes could be sensed by the smartphone, i.e., multiple ranging and relative direction results, the accuracy of the location estimation result could be further improved and optimized via multiple constraints.

B. System Design

In this paper, we design *opportunistic sensing* scheme that involves Bluetooth-Low-Energy (BLE) based received-signal-strength (RSS) ranging, acoustic-based angle measurement, relative Time-of-Arrival (TOA) ranging, displacement and moving direction estimation, processing and fusing hybrid data, and adapt to centimeter accuracy with sufficient measurements. We propose a smartphone-based indoor localization system using our newly designed low-complexity anchor node, because opportunistic sensing will never succeed without adequate anchor node as sensing source.

1) Anchor Node Design: We select the BLE and acoustic signal as the two main beacon signal types. The BLE signal is low-power and high efficiency in terms of RSS scanning compared to WiFi; it is also the reason that Apple and Qualcomm all select BLE as the main beacon source [7], [8]. Due to the strong promotion force by these industry leaders, and the convenient iBeacon APIs introduced in iOS7 [7], we propose to design anchor node that could support Apple's iBeacon specification.

We design the low-complexity anchor node from scratch to lower the overall cost and meet our long-term objective. The overall bill of material (BOM) price is kept lower than $20 for low cost and potential for wider availability. The system architecture is shown in Fig. 1 with three important parts: BLE radio, microcontroller, and audio codec. The power system is designed to adapt power from multiple sources, i.e., micro-USB, lithium battery and solar-panel.

To fast deploy the developed algorithm, we designed a back-end server for processing complex algorithms without worrying the limited resources on the mobile platform. A Redis server [9] is used as a cloud key-value store for the smartphone; A Java server performs computation for the structured data in the Redis server. The smartphone performs sensing and estimation of the raw data, with result data (small size) upload to server for complex algorithm processing. This approach balances computation and network consumption in a smartphone, and the introduced delay is less than $100ms$, which is ignorable for the sub-second level location update rate.

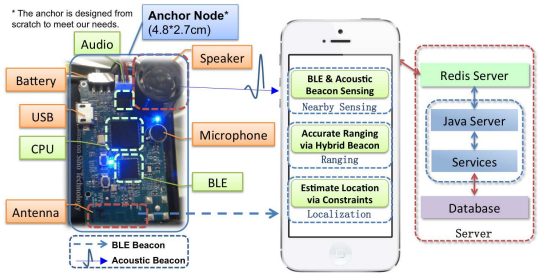

Fig. 1. System Architecture.

III. Localization with Less Anchors

In the most simple case, one anchor node provides basic check-in services, and coarse-grained location estimation. To improve the accuracy, we utilize the acoustic RSS and TOA ranging for distance measure, INS for displacement and direction estimation, and leverage the activity measurement for error mitigation. To support multiple user simultaneously, all the ranging process is in one-way passive mode, in which the smartphone only needs to receive beacons. Thus, the high accurate TOA result is the pseudorange between the smartphone and anchor pair. The inertial sensors, i.e., Accelerometer and Gyroscope, are utilized for accurate displacement and direction estimation.

When utilizing the omnidirectional ranging information with the single anchor node, the performance improvement is limited if the rough direction is unknown. To estimate the direction, BLE signal needs an expensive directional antenna; while the speaker of acoustic signal is mostly directional. Thus, combining BLE and acoustic for ranging could be an economical way to obtain coarse-grained distance and angle. Another benefit comes from the acoustic TOA estimation result, which is beneficial if the user start moving under single anchor coverage.

A. BLE and Acoustic Ranging

1) Acoustic TOA Based Ranging: TOA based ranging approaches rely on the delay estimation of the beacon signal from the anchor node to the mobile phone. Based on [4], we design

acoustic one-way TOA ranging approaches to support multiple users simultaneously, and make the beacon signal unnoticeable to human's ear. Leveraging the DAC and miniDSP module in our audio chip, we generate designed signal waveform and perform correlation in the receiver for better robustness, rather than the simple sharp pulse used in [4]. The smartphone samples the acoustic beacon in full resolution, and obtain the channel response in full detail.

By detecting the first path in the channel response, the delay and energy of the first path is the TOA (t_m) and RSS value (ε_m^r). The obtained TOA ranging measurement $\tilde{r}_{n,m}$ for the n-th user from the m-th anchor can be modeled as

$$\tilde{r}_{n,m} = \underbrace{\delta_m + v_s(f_n - f_m)t_m/F_s}_{\text{clock drift}} + \underbrace{\left(v_{n,m}^p + v_s\right) t_m + a_{n,m}^p t_m^2}_{\text{user movement}} \tag{1}$$

where δ_m is the unknown bias for the m-th anchor node that maps the $\tilde{r}_{n,m}$ to the real distance; t_m is the TOA time for the m-th anchor; $(f_n - f_m)$ is the clock frequency drift between the n-th mobile phone (f_n) and m-th anchor node (f_m); $v_{n,m}^p$ and $a_{n,m}^p$ are the projected moving speed and acceleration of the n-th user in the direction to the m-th anchor. v_s is the speed of the acoustic signal; F_s is the sampling rate of the mobile phone. The first part of (1) is contributed by the clock drift, and can be approximated as a linear function to the time t_m; the second part is contributed by the user movement, and becomes a curve (second or third order) when the user is moving.

2) RSS Based Ranging: One drawback of the one-way TOA-based ranging lies in its relative measurement feature, i.e., the bias caused by clock drift in (1) is unknown. To obtain the absolute distance measurement, we can direct utilize the acoustic and BLE RSS for coarse-grained ranging, then apply the fine-grained relative TOA distance as a constraint when the user is moving.

The RSS from BLE is calculated at the packet level, where the energy is averaged over all multi-path components. Using the BLE RSS for ranging, we could obtain fast energy scan in low cost, e.g., micro-second level scanning time for the BLE signal in iOS platform, while WiFi scan takes nearly one second and even not allowed by Apple.

Compared with the RSS value obtained from BLE signal, the RSS from the acoustic beacon of the anchor node is more accurate and sensitive, especially in short range and LOS condition. Moreover, the full channel impulse response is available in our acoustic ranging system, we can obtain the signal energy (ε_m^r) of the TOA path as the RSS, which is more precise and shows better robustness to multi-paths in indoor complex environments.

To model the RSS attenuation curve as the distance changes, we conduct experiments to measure the RSS of the acoustic signal and BLE signal by changing the distance of the anchor and the mobile phone pair from $1.5 \sim 20$ meters with the step size of 0.762 meters. The obtained RSS attenuation curve from BLE signal and acoustic signal are shown in Fig. 2. The RSS value of the BLE signal in Fig. 2a is obtained by using our anchor node and Apple iPod Touch 5 as the beacon, respectively. For acoustic ranging approach, the RSS result in Fig. 2b shows strong monotonicity due to the fine-grained channel measurement of the TOA path, which contributes to better ranging accuracy.

Using the power law function to fit the RSS attenuation data, the fitted curve can be modeled as $rss(d) = 0.0115d^{-1.199}$, where d is the distance. In real cases, the RSS ranging could be realized by measuring the current RSS value rss, and input the rss into the inverse function of $rss(d)$, where the distance can be calculated by $d = (rss/0.0115)^{-0.834}$.

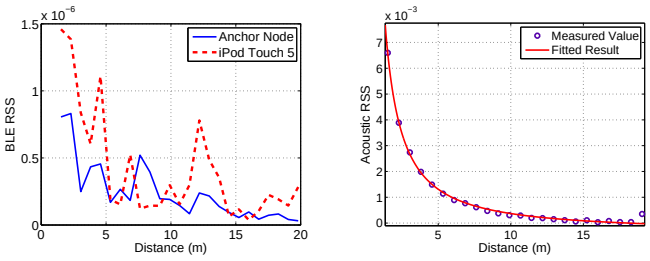

(a) BLE Ranging (b) Acoustic Ranging

Fig. 2. The RSS attenuation model for ranging when using: (a) Bluetooth-Low-Energy (BLE) signal; (b) the TOA path of acoustic signal.

Although the RSS ranging result from acoustic beacon is more accurate, the coverage and the NLOS robustness are still worse than BLE beacon. If the received TOA RSS is unavailable, the RSS ranging result should be replaced by the BLE RSS ranging value. Thus, the RSS ranging result $\hat{r}_{n,m}^{(k)}$ is a combined value from BLE and acoustic signal.

B. Displacement Estimation

To estimate the relative translation ($\mathbf{t}$) of the smartphone, we could utilize the Accelerometer on-board by measuring its force, acceleration, and infer the displacement by double integrating the acceleration. The quantity result from Accelerometer is the acceleration rate in m/s^2, and can be denoted as $\mathbf{f}_t^b = (f_t^{b_x}, f_t^{b_y}, f_t^{b_z})^T$, where $f_t^{b_{x,y,z}}$ is the measured force in 3-axis directions in the *body* frame.

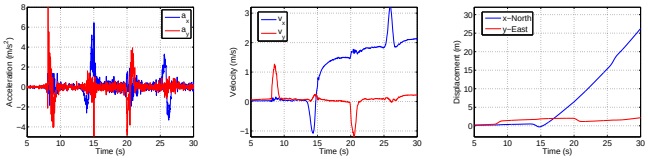

(a) Acceleration (b) Velocity (c) Displacement

Fig. 3. Motion estimation result via conventional method: (a) acceleration, (b) velocity, (c) displacement.

Direct integrates $\mathbf{f}_t^b$, obtains the displacement in the *body* coordinate, which is not related to the real geodesic displacement. To convert the obtained acceleration of the smartphone to the local *navigation* coordinate, we could apply rotation and translation over $\mathbf{f}_t^b$ by

$$\mathbf{f}_t^n = \mathbf{R}_b^n \mathbf{f}_t^b + \mathbf{e}^n \tag{2}$$

where $\mathbf{e}^n$ is the error of the force that applied to the smartphone. $\mathbf{R}_b^n$ is the rotation matrix used to convert the coordinate, which can be directly accessed from mobile OS [10]. To obtain the acceleration caused by the applied forces, gravity should be subtracted by $\mathbf{a}_t^n = \mathbf{f}_t^n - \mathbf{g}$, where $\mathbf{g} = [0, 0, g]$ is the gravity vector. The measured acceleration result after gravity subtraction is shown in Fig. 3a.

After the denoising process, the velocity of the smartphone can be obtained by $\mathbf{v}_t^n = \mathbf{v}_0^n + \int_0^t \mathbf{a}_t^n$ as shown in Fig. 3b. From Fig. 3b, we know that the velocity is drift even when the user is in stationary.

The displacement can be calculated by $\mathbf{s}_t^n = \mathbf{s}_0^n + \int_0^t \mathbf{v}_t^n$, where $\mathbf{v}_0^n$, and $\mathbf{s}_0^n$ are the initial velocity and displacement. The result of estimated displacement in x and y direction is shown in Fig. 3b with large drift.

The process of obtaining relative displacement $\mathbf{s}_t^n$ is contributed by double integration, in which the measurement noise, i.e., $\int\int \mathbf{e}^n$, is also integrated and amplified. The white noise in acceleration measurements is integrated *twice* and causes a second-order random walk in displacement of the smartphone. As a result, bias errors cause errors in position that grow proportional to t^2. The error of the accelerometer measurement can be modeled as

$$\dot{\delta} = -\frac{1}{T_a}\delta + \mathbf{w_a} \tag{3}$$

where T_a is the correlation time of the accelerometer. The value of the T_a differs from different devices, and need to be estimated prior to calibration. $\mathbf{w_a}$ is the modeled Gaussian white noise.

C. Mitigating Displacement Estimation Error

Performing moving pattern extraction before integration could be a feasible way. The normal movement model could not be applied to estimating the human's moving, e.g., we cannot walk at constant velocity (CV) or constant acceleration (CA) like a vehicle or a plane. Human's walking or movement has its own pattern, and we need to "accelerate" and "decelerate", then "accelerate" for another footstep. Here we use "start-moving-stop" movement model.

Performing "start-moving-stop" pattern decomposition could help us estimate the displacement in a more meaningful way. Using start, acceleration, deceleration and stop as one basic step, the velocity changes (from zero to top to zero) can be modeled as a Gaussian shape $g_v(\mu, \sigma) = \pm\exp\{-(x-\mu)^2/(2\sigma^2)\}$, where $+$ means moving forward; $-$ means backward. The acceleration is the derivative of the velocity, i.e., $g_a(\mu, \sigma) = \pm(x-\mu)/\sigma^2 \exp\{-(x-\mu)^2/(2\sigma^2)\}$. Using $g_a(\mu, \sigma)$ as the *kernel* function, we can decompose the acceleration measurement $\mathbf{a}_t^n$ into a series of $\eta g_a(\mu, \sigma)$ with different parameters η, μ and σ. Then the decomposed series of acceleration is $\sum_{i=1}^{n} \eta_i g_a(\mu_i, \sigma_i)$, η_i is the amplitude of each Gaussian derivative pulse. The fitting process can be modeled as

$$\{\eta_i, \mu_i, \sigma_i\} = \min_{\{\eta_i, \mu_i, \sigma_i\}} ||\mathbf{a}_t^n - \eta_i g_a(\mu_i, \sigma_i)|| \tag{4}$$

To reduce the number of parameters during the fitting process, we extract the feature points of $\mathbf{a}_t^n$, e.g., peak position and width, by thresholding the peak maximum and rising edge. Then we use the number of peaks found and the peak positions and widths to fit the specified peak model. This combination yields better and faster computation, and deals with overlapped peaks as well. During the decomposition and fitting process, the sign of η_i is determined by comparing the remaining error of using positive and negative results.

D. Improving the Location Robustness via Constraints

With the acoustic ranging results and the displacement and direction estimation, we perform location optimization to the initial location even with single anchor.

1) Initial Location: The initial location of smartphone could be accessed by directly using the API provided by mobile operating system. The obtained initial location is at Geodetic coordinates (latitude ϕ, longitude λ, height h), e.g., WGS 84 datum. To convert the Geodetic coordinates to the *navigation* coordinate, we first convert it to the earth-centered earth-fixed (ECEF) coordinate, then convert the ECEF to ENU frame. By subtracting the reference point O_R, the GPS location is mapped to the *navigation* coordinate (n-frame) for more intuitive and practical analysis. Define the POI's 3D position as $\mathbf{x}_i^n = [x_i^n, y_i^n, z_i^n]^T$, where the superscript n denotes the position value in the *navigation* coordinate; i denotes the i-th POI in M POIs ($i = 0, M-1$). The current location of the smartphone is defined as $\mathbf{p}^n = [x^n, y^n, z^n]^T$.

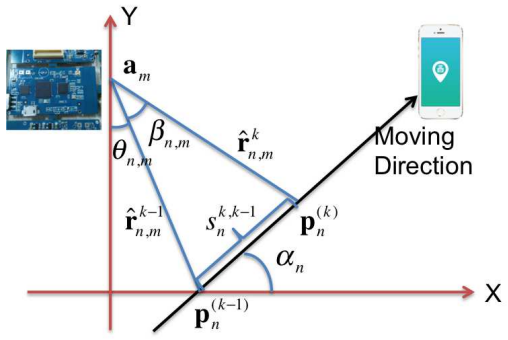

Fig. 4. Location Estimation via Single Anchor.

2) Ranging, direction, and angle constraints: Assume the position coordinate of the anchor node is $\mathbf{a}_m \in \mathbb{R}^d$, where m is the index of total M anchor nodes. For 2-D coordinate ($d = 2$), $\mathbf{a}_m$ is $[x_m, y_m]^T$, $m = 1, \ldots, M$. Denote the location coordinate of the n-th user is $\mathbf{p}_n$, $n = 1, \ldots, N$.

To refine the user's location, ranging information is utilized as a constraint. Assume the initial position coordinate of a user obtained by smartphone is $\hat{\mathbf{p}}_n$, which is direct from location API and low-accurate compared to the location of anchor nodes ($\mathbf{a}_m$). Defining the RSS ranging measurement between the user and anchor pair is $\hat{r}_{n,m}$; the estimated relative TOA distance is $\tilde{r}_{n,m}$. The real distance $r_{n,m}$ from the n-th mobile phone to the m-th anchor node is written as $r_{n,m} = ||\mathbf{p}_n - \mathbf{a}_m||_2$, where $||\cdot||_2$ calculates the 2-norm and

obtains the Euclidean distance. The vector form of the RSS ranging observation from m-th anchor to n-th mobile phone can be written as

$$\hat{\mathbf{r}}_{n,m} = ||\mathbf{p}_n - \mathbf{a}_m||_2 + \hat{\mathbf{n}}_{n,m} \tag{5}$$

where $\hat{\mathbf{n}}_{n,m}$ is the measurement noise; $m = 1, \cdots, N^B$. Then, the TOA distance measure from m-th anchor to n-th mobile phone is

$$\tilde{\mathbf{r}}_{n,m} = ||\mathbf{p}_n - \mathbf{a}_m||_2 + \delta_{n,m} + \mathbf{n}_{n,m} \tag{6}$$

where $\mathbf{n}_{n,m}$ is the TOA measurement noise, which is lower than $\hat{\mathbf{n}}_{n,m}$ in (5). $m = 1, \cdots, N^A$, where $N^A \leq N^B$. $\delta_{n,m}$ is the unknown bias between the m-th anchor and n-th mobile phone pair due to the unsynchronized clock. Thus, TOA result (6) is the relative distance measured between the smartphone and anchor.

The obtained displacement could be another measurement that contributes to the location optimization. For k and $k+1$ measurements, the displacement can be written as

$$s_n^{k,k-1} = ||\mathbf{p}_n^{(k)} - \mathbf{p}_n^{(k-1)}||_2 + \mathbf{n}_s \tag{7}$$

The direction of the motion traces obtained from the altitude value is assumed as α_n as shown in Fig. 4. With the RSS ranging results and TOA relative ranging results from the anchor to the smartphone, the anchor related measurement could be written as

$$\begin{aligned} \hat{\mathbf{r}}_{n,m}^{k-1}\cos(\theta_{n,m}) - \hat{\mathbf{r}}_{n,m}^{k}\cos(\theta_{n,m} + \beta_{n,m}) \\ = s_n^{k,k-1}\sin(\alpha_n) + \mathbf{n}_A \end{aligned} \tag{8}$$

where the angle $\beta_{n,m}$ could be calculated by the law of cosines. The geometric relation is shown in Fig. 4.

$\theta_{n,m}$ is the *angle* measurement information. When the user moves into the acoustic beacon coverage, the rough value of $\theta_{n,m}$ is related to the anchor installation direction, which is known. $\theta_{n,m}$ is also related to the location difference of $\mathbf{p}_n = [p_x, p_y]$ and $\mathbf{a}_m = [a_x, a_y]$, with its x and y coordinate related by $p_x = a_x + \hat{\mathbf{r}}_{n,m}^{k-1}\sin(\theta_{n,m})$ and $p_y = a_y - \hat{\mathbf{r}}_{n,m}^{k-1}\cos(\theta_{n,m})$. Due the wide beam of the acoustic speaker, the accuracy of $\theta_{n,m}$ is not high. This is the inherent limitation of (8). However, the error surface reduction is significant when compared with the case that the angle is not utilized.

3) Location Optimization: Thus, the location optimization problem when the anchor node number is insufficient for trilateration can be defined by using (5), (6), (7), and (8) to obtain a refined result of $\mathbf{p}_n$.

For the k-th iteration, the position refinement process is achieved by minimizing the error term of adjacent measurements $\mathbf{p}_{n,m}^{(k)}$ and $\mathbf{p}_{n,m}^{(k-1)}$ for all the received anchor nodes as

$$\mathbf{p}_n^{(k)} := \arg\min_{\mathbf{p}_n^{(k)} \in \mathbb{R}} \sum_{m \in \xi_M} \mathbf{e}\left(\mathbf{p}_n^{(k)}, \mathbf{p}_n^{(k-1)}\right) \tag{9}$$

where ξ_M is the set of all the received anchor nodes; when there is only one anchor node in the coverage area, then $m = 1$. The error term $\mathbf{e}(\mathbf{p}_n^{(k)}, \mathbf{p}_n^{(k-1)})$ illustrates the residual error between the measured distance and the calculated distance of the position coordinates (anchor and mobile phone). The introduced term $\mathbf{p}_n^{(k-1)}$ is to improve accuracy by leveraging the high accurate relative TOA measurements and estimated moving direction. By refining the search region of $\mathbf{p}_n^k$ within the region $\mathbb{R}$, some local optimum values that outside the real region could be avoided. Such refinement could significantly minimize large errors caused by insufficient and inaccurate measurements.

Considering all the available measurements, the error constraints between the current and previous $(k-1)$-th term $\mathbf{e}(\mathbf{p}_n^{(k)}, \mathbf{p}_n^{(k-1)})$ can be written as

$$\mathbf{e}(\mathbf{p}_n^{(k)}, \mathbf{p}_n^{(k-1)}) = (\gamma_1\mathbf{e}_S + \gamma_2\mathbf{e}_D + \gamma_3\mathbf{e}_M + \gamma_4\mathbf{e}_A) \tag{10}$$

where $\mathbf{e}_S$ and $\mathbf{e}_D$ means the remaining error term of the RSS and relative TOA in (5) and (6). $\mathbf{e}_M$ and $\mathbf{e}_A$ is the remaining error of (7) and (8), respectively. γ_1, γ_2, γ_3 and γ_4 are weighting coefficients that control the contribution of different measurements.

Perform the gradient operation ∇ to the error residues $\mathbf{e}(\mathbf{p}_{n,m}^{(k)}, \mathbf{p}_{n,m}^{(k-1)})$ with respect to the anchor node m, the refined position can be updated via the steepest descent approach by

$$\mathbf{p}_n^{(k)} := \hat{\mathbf{p}}_n^{(k)} + \alpha\nabla \sum_{m \in \xi_M} (\gamma_1\mathbf{e}_S + \gamma_2\mathbf{e}_D + \gamma_3\mathbf{e}_M + \gamma_4\mathbf{e}_A) \tag{11}$$

where $\alpha \in (0, 1]$ is the update step size to control the convergence rate; ξ_M is the total received anchor nodes, where the number is insufficient for trilateration.

Substituting measurements into (11), $\mathbf{p}_n^{(k)}$ can be optimized and updated by leveraging the RSS and TOA ranging measurements. (11) starts with the initial coarse-grained location result $\hat{\mathbf{p}}_n^{(k)}$, and optimizes the location result by substituting the initial value of $\mathbf{p}_n^{(k)}$ by $\hat{\mathbf{p}}_n^{(k)}$.

IV. Trilateration via Semidefinite Programming

When there are multiple measurements from different anchor nodes, a fine-grained location result could be obtained by aggregating all the available information together. However, one thing that we need to be careful is adding bad measurement into our data pool would downgrade the overall performance, and may cause the estimation algorithm diverge if not handled appropriately.

To prevent the location estimation algorithm from diverging or converging to the local optimality, the concept of relaxation onto convex sets has been proposed [11]. Without the requirement of performing the inverse operation on the Jacobian matrix in LS-based approaches, SDP-based approach achieves better computational efficiency by leveraging existing SDP packages, which is especially important when the Jacobian matrix in LS problem is badly scaled or close to singular. Existing SDP algorithm mainly used for sensor network localization applications, where the key principle is leveraging multiple nodes and their relative distance measurements to optimize the overall location accuracy. However, our application demand is different. We need to leverage multiple data source rather than

multiple nodes. In this section, we propose an optimized real-time SDP algorithm in mobile phone location estimation. The proposed algorithm is robust in the presence of outliers by leveraging the delay-constraint, and Huber M-estimator [12].

A. Min-max Criterion

The location estimation process is a *nonconvex* optimization problem. While semidefinite programming (SDP) technique can be used to relax the initial *nonconvex* problem into convex one. Among existing relaxation criteria, *min-max* approximation and semidefinite relaxation can find the global minimum value without the "inside convex hull" requirement [11]. To utilize the SDP relaxation, we modify the problem formulation into $\hat{\mathbf{r}} - \delta_r = ||\mathbf{p} - \mathbf{a}_m||_2 + \mathbf{n}$. Performing a square operation on both sides leads to

$$(\hat{\mathbf{r}} - \delta_r)^T \mathbf{\Sigma}^{-1} (\hat{\mathbf{r}} - \delta_r) = (||\mathbf{p} - \mathbf{a}_m||_2 + \mathbf{n})^2 \qquad (12)$$

where the right side of (12) is $||\mathbf{p}-\mathbf{a}_m||_2^2 + 2\mathbf{n}^T||\mathbf{p}-\mathbf{a}_m||_2 + \mathbf{n}^T\mathbf{n}$. By adopting the *min-max* criterion [11], (12) can be formulated as

$$\mathbf{p} = \arg\min_{\mathbf{p}} \max_{m=1,\ldots,M} \underbrace{\left| ||\mathbf{p} - \mathbf{a}_m||_2^2 - (\hat{\mathbf{r}} - \delta_r)^T \mathbf{\Sigma}^{-1} (\hat{\mathbf{r}} - \delta_r) \right|}_{\xi} \qquad (13)$$

where the term ξ can be viewed as the residual error. (13) calculates $\mathbf{y}$ that corresponds to the minimum value of the maximum residual error. (13) remains nonconvex, but it is comfortable for the following semidefinite relaxations.

The first term in ξ can be written into a matrix form of

$$\begin{aligned} ||\mathbf{p} - \mathbf{a}_m||_2^2 &= \begin{bmatrix} \mathbf{p}^T & 1 \end{bmatrix} \begin{bmatrix} \mathbf{I}_d & -\mathbf{a}_m \\ -\mathbf{a}_m^T & \mathbf{a}_m^T \mathbf{a}_m \end{bmatrix} \begin{bmatrix} \mathbf{p} \\ 1 \end{bmatrix} \qquad (14) \\ &= \text{trace} \left\{ \begin{bmatrix} \mathbf{p} \\ 1 \end{bmatrix} \begin{bmatrix} \mathbf{y}^T & 1 \end{bmatrix} \begin{bmatrix} \mathbf{I}_d & -\mathbf{a}_m \\ -\mathbf{a}_m^T & \mathbf{a}_m^T \mathbf{a}_m \end{bmatrix} \right\} \\ &= \text{trace} \left\{ \begin{bmatrix} \mathbf{P} & \mathbf{p} \\ \mathbf{p}^T & 1 \end{bmatrix} \begin{bmatrix} \mathbf{I}_d & -\mathbf{a}_m \\ -\mathbf{x}_m^T & \mathbf{a}_m^T \mathbf{a}_m \end{bmatrix} \right\} \end{aligned}$$

where $\mathbf{P} = \mathbf{p}\mathbf{p}^T$, $\text{trace}\{\cdot\}$ calculates the trace of the matrix, $\mathbf{I}_d$ is an identity matrix of order d. Following the same process in (14), the second term in ξ can be written into

$$\begin{aligned} &(\hat{\mathbf{r}} - \delta_r)^T \mathbf{\Sigma}^{-1} (\hat{\mathbf{r}} - \delta_r) \qquad (15) \\ &= \text{trace} \left\{ \begin{bmatrix} \mathbf{\Delta} & \delta_r \\ \delta_r^T & 1 \end{bmatrix} \begin{bmatrix} \mathbf{\Sigma}^{-1}\mathbf{I}_d & -\mathbf{\Sigma}^{-1}\hat{\mathbf{r}} \\ -\hat{\mathbf{r}}^T\mathbf{\Sigma}^{-1} & \hat{\mathbf{r}}^T\mathbf{\Sigma}^{-1}\hat{\mathbf{r}} \end{bmatrix} \right\} \end{aligned}$$

where $\mathbf{\Delta} = \delta_r \delta_r^T$.

B. Delay-Constraint Robust Semidefinite Programming

From (1), we know that the unknown parameter δ_r incorporates the unknown clock drift. The trend of δ_r is known as a line and the future value can be directly estimated, e.g., by linear fitting. Using such prior information, the location estimation accuracy can be further improved by substituting this pre-estimated delay δ_r as a constraint; we name this approach as delay constraint (DC).

The objective function of ξ can be converted to minimize ϵ at the constraint of an inequality expression $-\epsilon < \xi < \epsilon$, while ξ can be written as the form of (14) and (15). However, the outliers could not be ignored during location estimation. One possible solution is to apply a penalty function to the residual error rather than only using the quartic term (l_2-norm). Specifically, we still apply l_2-norm on any residual smaller than a preset threshold σ_{th}, but put a linear weight (reverts to l_1-like linear growth) on any residual larger than σ_{th}. Using l_1-norm for large errors would lower the weight for outliers and improve the robustness. We choose Huber function $\theta_{hub}(\varepsilon)$ as the penalty function [13]. This penalty function can be considered as a convex approximation of other outlier penalty functions. The constraints form of (14) and (15) are convex, but the equality constraints of $\mathbf{P} = \mathbf{p}\mathbf{p}^T$ and $\mathbf{\Delta} = \delta_r \delta_r^T$ are nonconvex. Using semidefinite relaxation, these two equalities can be relaxed to inequality constraints of $\mathbf{P} \succeq \mathbf{p}\mathbf{p}^T$ and $\mathbf{\Delta} \succeq \delta_r \delta_r^T$, respectively. The matrix form of these two equalities is

$$\begin{bmatrix} \mathbf{P} & \mathbf{p} \\ \mathbf{p}^T & 1 \end{bmatrix} \succeq 0, \quad \begin{bmatrix} \mathbf{\Delta} & \delta_r \\ \delta_r^T & 1 \end{bmatrix} \succeq 0 \qquad (16)$$

where $\succeq$ means a positive definite (semidefinite) matrix, which is different from $\geq$.

Accordingly, the initial localization problem can be relaxed to a semidefinite programming form as

$$\begin{aligned} &\min\nolimits_{\{\mathbf{p},\mathbf{P},\delta_r,\mathbf{\Delta}\}} \theta_{hub}(\epsilon) \\ \text{s.t.} \quad &-\theta_{hub}(\epsilon) < \text{trace} \left\{ \begin{bmatrix} \mathbf{P} & \mathbf{p} \\ \mathbf{p}^T & 1 \end{bmatrix} \begin{bmatrix} \mathbf{I}_d & -\mathbf{a}_m \\ -\mathbf{a}_m^T & \mathbf{a}_m^T \mathbf{a}_m \end{bmatrix} \right\} - \\ &\text{trace} \left\{ \begin{bmatrix} \mathbf{\Delta} & \delta_r \\ \delta_r^T & 1 \end{bmatrix} \begin{bmatrix} \mathbf{\Sigma}^{-1}\mathbf{I}_d & -\mathbf{\Sigma}^{-1}\hat{\mathbf{r}} \\ -\hat{\mathbf{r}}^T\mathbf{\Sigma}^{-1} & \hat{\mathbf{r}}^T\mathbf{\Sigma}^{-1}\hat{\mathbf{r}} \end{bmatrix} \right\} < \theta_{hub}(\epsilon), \\ &m = 1, \ldots, M, \\ &\begin{bmatrix} \mathbf{P} & \mathbf{p} \\ \mathbf{p}^T & 1 \end{bmatrix} \succeq 0, \quad \begin{bmatrix} \mathbf{\Delta} & \delta_r \\ \delta_r^T & 1 \end{bmatrix} \succeq 0 \\ &\hat{\delta}_r(1-\alpha) < \delta_r < \hat{\delta}_r(1+\alpha) \end{aligned}$$

where $\hat{\delta}_r$ is the estimated delay value based on historical data of δ_r; α is predefined and used to relax the delay-constraint (DC). The n-th mobile phone position $\mathbf{p}$ can be extracted from the optimal solution of $\{\mathbf{p}, \mathbf{P}, \delta_r, \mathbf{\Delta}\}$. This delay-constraint robust SDP problem can be solved by some standard convex optimization packages, e.g., SeDuMi. By using the steepest descent approach in (11), the estimation error can be further reduced by performing a local search above the global optimized value obtained by SDP.

V. Evaluation

A. Experiment Setting

Besides the implementation in a smartphone, we designed the acoustic anchor node for indoor localization purpose. The maximum operating distance for one anchor node is near 20 meters. In the following system evaluation, we deployed 8 anchor nodes in one large exhibition room of our campus Art

TABLE I
PERFORMANCE COMPARISON WITH RESPECT TO DIFFERENT METHODS UNDER SPECIFIC METRICS

Methods	Metrics	Average	Median
Basic	Total Drift (m)	16.51	12.47
	Drift Speed (m/s)	0.47	0.40
	Drift Rate (m/m)	3.92	3.73
Velocity Calibration [14]	Total Drift (m)	1.26	1.02
	Drift Speed (m/s)	0.04	0.04
	Drift Rate (m/m)	0.31	0.26
Proposed SMS approach	Total Drift (m)	0.23	0.14
	Drift Speed (m/s)	0.006	0.0045
	Drift Rate (m/m)	0.055	0.043

Museum as shown in Fig. 5. Enriching visiting experience in a museum is one of the promising applications of indoor localization.

Fig. 5. Anchor deployment and experiment environment.

B. Displacement Estimation

To evaluate the drift reduction performance of our proposed INS displacement estimation algorithm, we compare our proposed approaches, i.e., start-moving-stop model (SMS). The performance metrics include: Total Drift, Drift Speed (drift per second), and Drift Rate (drift per meter).

Drift Metrics and Experiments. To reduce the randomness in performance evaluation, we tested more than 150 cases. The average and median values of all the metrics are shown in Table I. Our proposed SMS approach achieves best performance in all metrics. Different from the existing velocity calibration approach that performs binary moving detection and suppresses the non-moving drift to zero, our SMS approach is more genetic in terms of modeling the whole moving pattern rather than the simple binary decision. The drift rate of 5.5cm per meter is significantly better than existing approaches.

Drift Reduction. After applying the SMS approach for the results in Fig. 3, we could obtain better acceleration, velocity and displacement results as shown in Fig. 6. The ground truth of the moving path is like a rectangle, where the starting point and ending point is overlapped. The velocity is calibrated as multiple start-moving-stop pattern; the drift of the estimated displacement is significantly reduced (the starting point and end point show the same location value). With the x and y estimated together, the moving direction of the user in the 2-D *navigation* coordinate is also known.

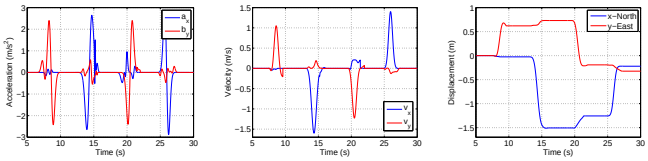

(a) Acceleration (b) Velocity (c) Displacement

Fig. 6. Motion estimation result via proposed method: (a) acceleration, (b) velocity, (c) displacement.

C. Ranging Results

To evaluate and quantify the RSS and TOA ranging performance, we conducted a series of ranging measurements by changing the relative distance of smartphone-anchor pair from 1.5m to 20m with the step size of 0.762m in the large exhibition room as shown in Fig. 5. Every measurement lasted more than 100 seconds to minimize randomness. The RSS ranging error is shown in Fig. 7a, where the accuracy degrades at large distances and the average accuracy is on the meter-level. The TOA ranging accuracy is significantly better than RSS ranging results as shown in Fig. 7b, and the average accuracy is in the centimeter-level. From Fig. 7a and Fig. 7b, we know that the operating distance of one anchor node is near $17 \sim 20$ meters, which is sufficient for covering one room in an indoor environment.

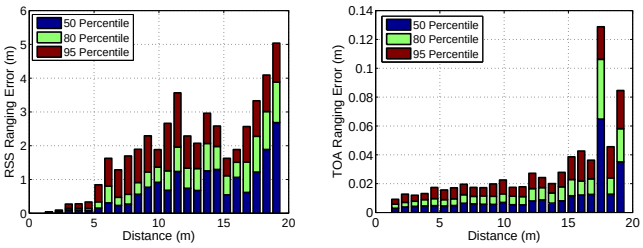

(a) RSS Ranging Error (b) TOA Ranging Error

Fig. 7. (a) RSS and (b) TOA ranging error.

D. Angle Measurement Results

To test the directional coverage or the angle of the BLE and acoustic RSS signal, we conduct experiments to measure the radiation beam of the BLE antenna and acoustic speaker as shown in Fig. 8a and Fig. 8b, respectively. The environment is the same to Fig. 5. There are some blockages caused by nearby exhibitions (the glass table). The measured RSS values in different angles (0^o to 360^o) are normalized. Compared with the almost omnidirectional radiation of the BLE beacon, acoustic beacon has high directionality, which contributes to its angle estimation features.

E. Improving Location Accuracy with Less Anchors

To evaluate the performance improvement of our proposed algorithm when the anchor nodes are insufficient for trilateration, we conduct experiments using Apple iPhone5S in the

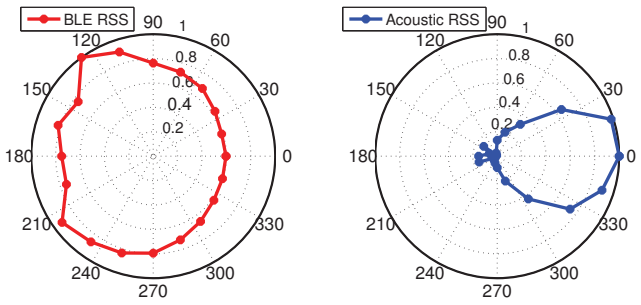

(a) BLE RSS (b) Acoustic RSS

Fig. 8. The polar distribution of normalized (a) BLE and (b) acoustic RSS for ranging.

museum environment. We randomly select 1 to 2 anchors from the total 8 anchors in Fig. 5 as 7 different configurations in the x-axis of Fig. 9. Fig. 9a is conducted when no anchor is blocked, i.e., the line-of-sight (LOS) case; Fig. 9b is conducted when one anchor is blocked, i.e., the non-line-of-sight (NLOS) case. To quantify the location performance and smooth out the random effect, we conducted measurements at 20 different location points for each configuration. And every location measurement contains more than 400 test results in each location point. We totally have 8000 results for each bar in Fig. 9. The 'initial' approach is based on state-of-the-art BLE-based localization (Apple's iBeacon), where there is no acoustic beacon received. The 'm=1, static' leverages the acoustic beacon from one anchor node; the 'm=2, Dynamic' leverages the one acoustic beacon plus the motion results.

As shown in Fig. 9, when the anchor number is $m = 1, 2$, our proposed approach could significantly improve the location accuracy compared with normal BLE-based localization. Applying the dynamic part of (11) by leveraging the relative TOA distance measurement and moving direction, the performance could be even improved as shown in the case of 'm=2, Dynamic'. From Fig. 9, we know that the accuracy improvement ranges from 2 to 11 times over the initial results.

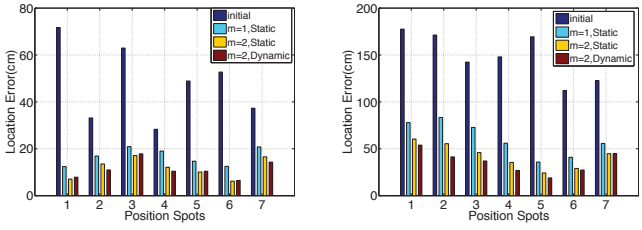

(a) LOS Results (b) NLOS Results

Fig. 9. The location error when the anchor number is $m = 0 \sim 2$ in (a) outdoor and (b) indoor environments.

F. Trilateration via Semidefinite Programming

To evaluate and compare the performance of different localization algorithms when there are more anchor nodes available, we randomly select 3, 4 and 5 anchors from all 8 anchors in Fig. 5, and average them together. To emulate the real application scenarios, the experimental environment is polluted with random voice sound and other acoustic interferences.

Performance Comparison. The algorithms compared are: "LS-Classic" [15], "LS-PR" [4], "SDP-PR" [16], "SDP-PR-DC" and "SDP-PR-DCR". Fig. 10a and Fig. 10b show the CDF of the position error when the mobile phone is in LOS and NLOS environment, respectively. The SDP-based approaches perform better than the LS-based approaches in all these two cases. By performing delay-constraint (DC) and robust (R) approach (using Huber Estimator) during the SDP optimization, "SDP-PR-DCR" outperforms other approaches in most situations with different performance gains.

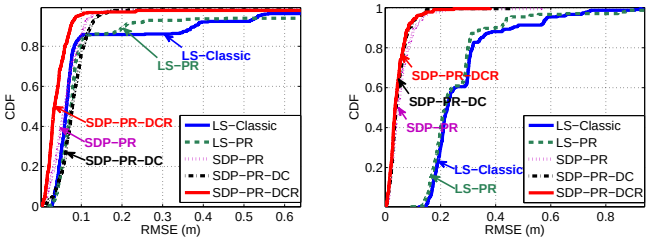

(a) LOS (b) NLOS

Fig. 10. Cumulative Distribution of different algorithms when the mobile phone is in: (a) LOS and (b) NLOS environment by averaging 40 cases with 3, 4 and 5 anchors.

Dynamic Performance over Time. To demonstrate the dynamic localization performance over time, we calculated the localization accuracy of "SDP-PR-DCR" when its user stands still at different location spots. To support quantitative analysis, we use the time series (Fig. 11a) and CDF (Fig. 11b) of the localization error to illustrate the performance. If using 80% probability, the localization errors for all the spots are in the range between $4cm$ to $10cm$. These results are very accurate for indoor mobile phone based localization.

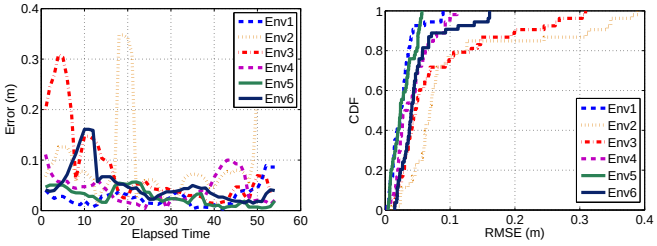

(a) Time Series (b) CDF

Fig. 11. (a) The time series and (b) CDF of location error at different spots with 6 anchors.

Moving Traces. Fig. 12 shows the location tracking traces of a smartphone when a user is in stationary and moving. These smooth moving traces of line and curve illustrate the effectiveness of tracking a user with sufficient accuracy and update rate.

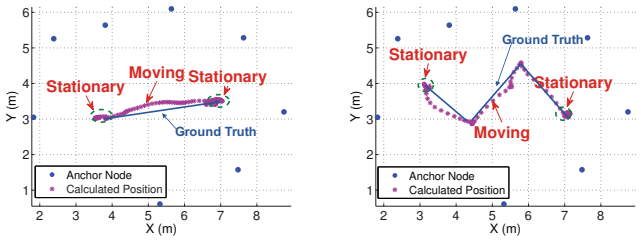

(a) Line (b) Curve

Fig. 12. Two tracking traces (a) line and (b) curve of a smartphone with 8 anchors.

VI. Related Work

Localization via anchor nodes: Recent approaches relying on the high-band of the microphone sensor introduces a convenient approach for trilateration without additional hardware attachment on user's smartphone [5], [15], [3], [4], [1], [17], [2]. Liu et al. [4] utilize low-complexity anchor nodes for broadcasting unnoticeable acoustic beacon in high accuracy. However, at least three anchor nodes are needed for one location calculation with 2-D coordinate, and more nodes are needed for covering large areas, which inhibits the wide deployment.

Localization via hybrid approaches: Leveraging multiple sensors in a mobile phone and optimizing the location accuracy via moving traces without anchor nodes is proposed in [18]. However, the moving traces obtained by an accelerometer and compass are inaccurate and highly depend on the prior information on the footstep length. Authors [19] proposed localization optimization approach via peer-to-peer ranging. However, the two-way ranging process between all users-pairs are too time-consuming and inconvenient. Rajalakshmi et al. [15] proposed systems named EchoBeep and DeafBeep that fusing RF and acoustic based techniques into a single framework. The requirement on the two-way ranging for EchoBeep and the triangular ranging for DeafBeep would limit the user numbers (only support one user) and introduce the complex ranging protocol and long delay, which is impractical in smartphone-based mobile system. SAIL [20] combines a physical layer (PHY) information and human motion for indoor localization using single Wi-Fi AP. However, the required Wi-Fi AP with PHY information is not ubiquitous.

VII. Conclusion

We proposed location optimization approaches in a mobile phone via opportunistic anchor sensing. Using the obtained coarse-grained absolute and fine-grained relative ranging information from accessible anchors, the location accuracy achieved significant improvement even with only one or two anchors. When sufficient anchors are available for trilateration, we proposed delay-constraint robust semidefinite programming to ensure robustness in the presence of ranging outliers. The achieved results show 2 to 11 times performance improvement with limited anchors, sub-second delay for supporting unlimited users, and achieve 80 percentile accuracy of $8cm$ with sufficient anchors.

References

[1] S. Kumar, S. Gil, D. Katabi, and D. Rus, "Accurate indoor localization with zero start-up cost," in *Proceedings of the 20th annual international conference on Mobile computing and networking*. ACM, 2014, pp. 483–494.

[2] Y. Wang, J. Liu, Y. Chen, M. Gruteser, J. Yang, and H. Liu, "E-eyes: device-free location-oriented activity identification using fine-grained wifi signatures," in *Proceedings of the 20th annual international conference on Mobile computing and networking*. ACM, 2014, pp. 617–628.

[3] P. Lazik and A. Rowe, "Indoor pseudo-ranging of mobile devices using ultrasonic chirps," in *Proceedings of the 10th ACM Conference on Embedded Network Sensor Systems*. ACM, 2012, pp. 99–112.

[4] K. Liu, X. Liu, and X. Li, "Guoguo: Enabling fine-grained indoor localization via smartphone," in *Proceedings of the 11th international conference on Mobile systems, applications, and services*. ACM, 2013.

[5] C. Peng, G. Shen, Y. Zhang, Y. Li, and K. Tan, "Beepbeep: a high accuracy acoustic ranging system using cots mobile devices," in *Proceedings of the 5th international conference on Embedded networked sensor systems*. ACM, 2007, pp. 1–14.

[6] N. Priyantha, A. Chakraborty, and H. Balakrishnan, "The cricket location-support system," in *Proceedings of the 6th annual international conference on Mobile computing and networking*. ACM, 2000, pp. 32–43.

[7] Apple ibeacon, en.wikipedia.org/wiki/ibeacon. [Online]. Available: en.wikipedia.org/wiki/IBeacon

[8] Qualcomm gimbal proximity beacon, http://www.qualcomm.com/solutions/gimbal. [Online]. Available: http://www.qualcomm.com/solutions/gimbal

[9] Redis.io. http://redis.io/. [Online]. Available: http://redis.io/

[10] Apple cmattitude. [Online]. Available: https://developer.apple.com

[11] C. Meng, Z. Ding, and S. Dasgupta, "A semidefinite programming approach to source localization in wireless sensor networks," *Signal Processing Letters, IEEE*, vol. 15, pp. 253–256, 2008.

[12] G.-L. Sun and W. Guo, "Bootstrapping m-estimators for reducing errors due to non-line-of-sight (nlos) propagation," *Communications Letters, IEEE*, vol. 8, no. 8, pp. 509–510, 2004.

[13] S. Boyd and L. Vandenberghe, *Convex optimization*. Cambridge Univ Pr, 2004.

[14] Y. Zou, G. Wang, K. Wu, and L. M. Ni, "Smartsensing: Sensing through walls with your smartphone!" in *Mobile Ad Hoc and Sensor Systems (MASS), 2014 IEEE 11th International Conference on*. IEEE, 2014, pp. 55–63.

[15] R. Nandakumar, K. Chintalapudi, and V. Padmanabhan, "Centaur: locating devices in an office environment," in *Proceedings of the 18th annual international conference on Mobile computing and networking*. ACM, 2012, pp. 281–292.

[16] P. Biswas, T. Liang, K. Toh, Y. Ye, and T. Wang, "Semidefinite programming approaches for sensor network localization with noisy distance measurements," *Automation Science and Engineering, IEEE Transactions on*, vol. 3, no. 4, pp. 360–371, 2006.

[17] Y. Zheng, G. Shen, L. Li, C. Zhao, M. Li, and F. Zhao, "Travi-navi: Self-deployable indoor navigation system," in *Proceedings of the 20th annual international conference on Mobile computing and networking*. ACM, 2014, pp. 471–482.

[18] Z. Yang, C. Wu, and Y. Liu, "Locating in fingerprint space: wireless indoor localization with little human intervention," in *Proceedings of the 18th annual international conference on Mobile computing and networking*. ACM, 2012, pp. 269–280.

[19] H. Liu, Y. Gan, J. Yang, S. Sidhom, Y. Wang, Y. Chen, and F. Ye, "Push the limit of wifi based localization for smartphones," in *Proceedings of the 18th annual international conference on Mobile computing and networking*. ACM, 2012, pp. 305–316.

[20] A. T. Mariakakis, S. Sen, J. Lee, and K.-H. Kim, "Sail: single access point-based indoor localization," in *Proceedings of the 12th annual international conference on Mobile systems, applications, and services*. ACM, 2014, pp. 315–328.